CORROSION SCIENCE AND TECHNOLOGY, Vol.3, No.3(2004), pp.118~126

Galvanic Sensor System for Detecting the Corrosion Damage of the Steel in Concrete

Jung-Gu Kim, Zin-Taek Park, Ji-Hong Yoo, and Woon-Suk Hwang*

Department of Advanced Materials Enginieering, Sungkyunkwan University, 300 Chunchun-Dong, Jangan-Gu, Suwon, 440-746, Korea
**School of Materials Science and Engineering, Inha University, Inchon, Korea*

The correlation between sensor output and corrosion rate of reinforcing steel was evaluated by laboratory electrochemical tests in saturated $Ca(OH)_2$ with 3.5 wt.% NaCl and confirmed in concrete environment. In this paper, two types of electrochemical probes were developed: galvanic cells containing of steel/copper and steel/stainless steel couples. Potentiodynamic test, weight loss measurement, monitoring of open-circuit potential, linear polarization resistance (LPR) measurement and electrochemical impedance spectroscopy (EIS) were used to evaluate the corrosion behavior of steel bar embedded in concrete. Also, galvanic current measurements were conducted to obtain the charge of sensor embedded in concrete.
In this study, steel/copper and steel/stainless steel sensors showed a good correlation in simulated concrete solution between sensor output and corrosion rate of steel bar. However, there was no linear relationship between steel/stainless steel sensor output and corrosion rate of steel bar in concrete environment due to the low galvanic current output. Thus, steel/copper sensor is a reliable corrosion monitoring sensor system which can detect corrosion rate of reinforcing steel in concrete structures.

Keywords *: galvanic sensor system, concrete, corrosion, pore solution, chloride*

1. Introduction

Reinforced concrete is a versatile, economical and successful construction material. It is durable and strong, performing well throughout its service life. However, the corrosion of reinforcing steel in concrete is becoming an issue in the collapse of the concrete structures as engineers and surveyors maintain an aging infrastructure in recent years. Usually, the steel embedded in concrete becomes passivated due to the initial high alkalinity ($12<pH<13$) of the pore solution. However, the protective film is destroyed and the reinforcing steel is depassivated when sufficient chloride ions (from de-icing salts or from seawater) have penetrated to the reinforcement or when the pH of the pore solution drops to low values due to carbonation. Corrosion in the form of rust formation and/or loss in cross section of the reinforcing steel occur in the presence of oxygen and water. The corrosion of steel in concrete essentially is an electrochemical process, where at the anode, iron is oxidized to iron ions that pass into solution and at the cathode, oxygen is reduced to hydroxyl ions. Anode and cathode form a short-circuited corrosion cell, with the flow of electrons in the steel and of ions in the pore solution of the concrete. The corrosion between actively corroding areas of the reinforcing steel and passive areas is of great concern because it results in very high local anodic current densities with corrosion rates up to 0.5-1 mm/year. The resulting local loss in cross section has dangerous implications for the structural safety if the corroded steels are located in a zone of high tensile or shear stresses.[1)-6)]

Many new systems and materials have been developed to delay the onset of corrosion and to increase durability. However, there is only limited success in delaying the time to corrosion. In view of economic and engineering points, quantitative assessment of corrosion is also important. Thereby, sensor systems are needed to enable owners of the structures to monitor the corrosion risk and to take protective measures before the damaging processes start. It must be more economical to remove and replace the areas of active reinforcement corrosion only, rather than to remove all the chloride-contaminated concrete, particularly in areas where active reinforcement corrosion had not started.[7)] However, techniques for inspection and monitoring of the corrosion of reinforcing steel in concrete structures are at present limited to either mechanical inspection, chemical analysis and/or iso-potential (half cell) mapping. In all cases these techniques can not supply

information on the corrosion rate occurring, but only provide information of the presence of corrosion.

The purpose of this research is to develop corrosion monitoring sensor system which can detect corrosion problems on a reinforced concrete structure quantitatively. It uses well-known principles of galvanic corrosion and consists of two dissimilar metals which provide current because of a natural voltage difference.

2. Experimental details

2.1 Tests in simulated concrete solution

2.1.1 Preparation for materials and solution

The anode material used in the present investigation was KS (Korean standards) D 3504 (steel bars for concrete reinforcement) with the chemical composition of 0.22 C, 0.14 Si, 0.59 Mn, 0.02 P, 0.025 S and balance Fe (in wt.%). Type 304 austenitic stainless steel (UNS S30400) and pure copper were used as the cathode materials. All specimens were machined in the shape of a bar with a diameter of 12 mm and polished with a 600 silicon carbide (SiC) grit emery paper. After grinding, the samples were ultrasonically cleaned, rinsed with ethanol and dried.

The electrochemical behavior of the specimens was examined under two conditions. First, the electrodes were immersed directly in saturated $Ca(OH)_2$ solution to reproduce the pore solution of concrete and secondly, the electrodes were immersed in saturated $Ca(OH)_2$ solution with 3.5 wt.% NaCl addition to represent environments of sufficient chloride ions (from de-icing salts or from seawater) penetrated to the real concrete environment.

2.2 Potentiodynamic polarization test

The potentiodynamic polarization tests were performed to evaluate the overall corrosion behavior of the anode and cathode materials. Measurements of electrochemical polarization were conducted using an EG&G 273A potentiostat. The electrochemical polarization cell consisted of a graphite counter electrode, a saturated calomel electrode (SCE) and the working electrode.

The potential of the sample was swept at a rate of 600 ㎷/h from the initial potential of -0.25 V vs. open circuit potential (OCP) to the final potential of +1.5 V vs. SCE. The experiments were started when the corrosion potential did not change by more than 1 ㎷/min within 20 min. The potentiodynamic tests were conducted at ambient laboratory temperature. The potentiodynamic data were used in Tafel extrapolation to calculate corrosion rates. All potentials are reported with respect to saturated calomel electrode (SCE). To insure reproducibility, at least three measurements were run for each specimen.

2.3 Immersion test

Immersion tests were conducted in saturated $Ca(OH)_2$ solution with 3.5 wt.% NaCl addition with the anode materials at ambient temperature and specimens were taken out from solution periodically. A concentrated hydrochloric acid solution was used to clean the corrosion products as described in ASTM G 1. Then, specimens were dried in an oven at 80℃ for 1h and weighed to 0.1 ㎎.

After the immersion test was completed, corrosion products on the metal surface were investigated by means of scanning electron microscopy (SEM) and X-ray photoelectron spectroscopy (XPS).

2.4 Galvanic corrosion test

Galvanic corrosion tests were accomplished in saturated $Ca(OH)_2$ solution with 3.5 wt.% NaCl addition with steel/copper and steel/stainless steel (Type 304) at ambient temperature. Galvanic current measurements were made with a zero-resistance ammeter. Fig. 1 shows the experimental arrangement. One electrode was connected to the working electrode (WE) terminal, the other to the reference electrode (REF) terminal which was connected to the auxiliary (AUX) electrode.

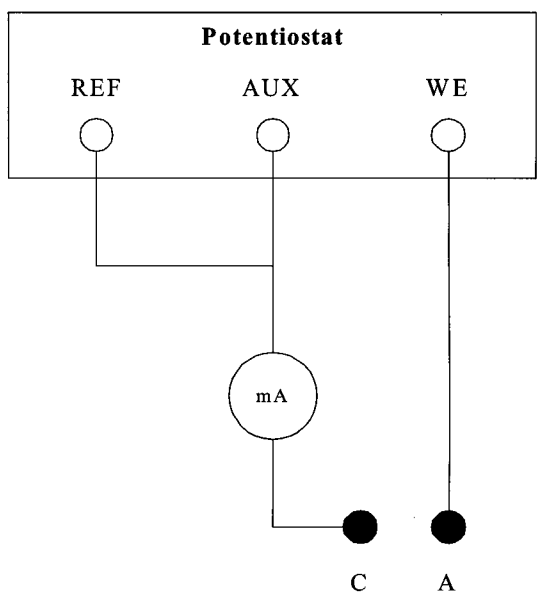

Fig. 1. Zero-resistance ammeter for measurement of galvanic current at shot circuit.

2.5 Tests in real concrete environment

2.5.1 Sensor system

Two types of corrosion detection sensors were designed, one for galvanic cell consisting of steel and copper electrodes, and the other for galvanic cell consisting of steel

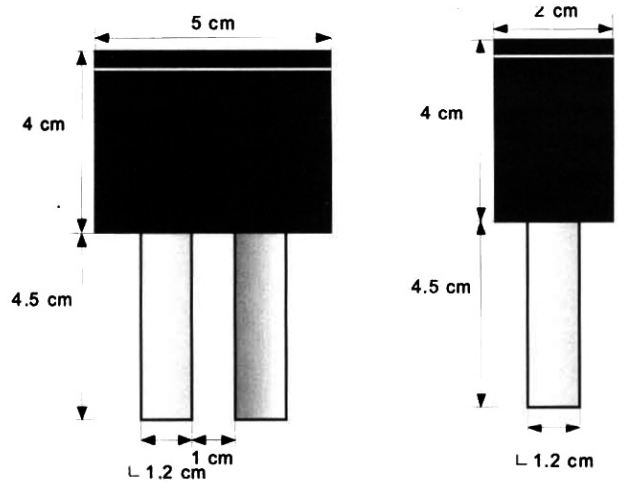

Fig. 2. Geometry of the galvanic sensor.

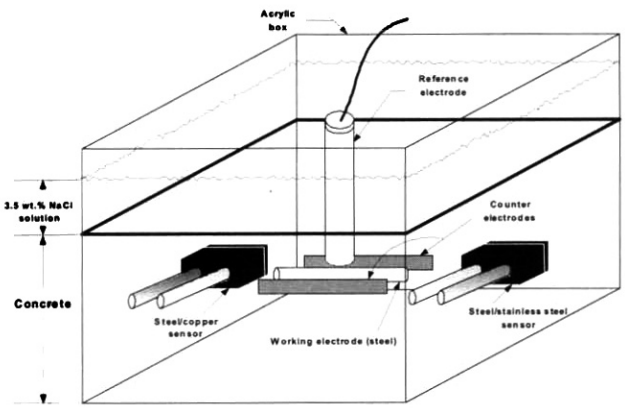

Fig. 3. Experimental setup of galvanic sensor system for electrochemical measurements.

and stainless steel electrodes. Geometry of corrosion detection sensor is schematically shown in Fig. 2. The anode material used in this investigation was steel bar for concrete reinforcement. Type 304 austenitic stainless steel (UNS S30400) and pure copper were used as the cathode materials.

To evaluate the correlation between sensor output and corrosion rate of reinforcing steel in concrete environment, sensor system was designed (Fig. 3). In the middle of designed acrylic cell, steel bar served as working electrode (WE) and there are high-purity graphite rods on both sides of the steel bar as counter electrode. All potential values were reported with respect to a copper/copper sulfate ($Cu/CuSO_4$) electrode (CSE) positioned in the center, right above steel bar. Two types of galvanic sensors, steel/copper and steel/stainless steel sensors, were placed in same height with steel bar.

2.5.2 Electrochemical testing

Electrochemical tests were conducted at designed sensor system under complete immersion in 3.5 wt.% NaCl solution. Open-circuit potential monitoring, linear polarization resistance measurement and electrochemical impedance spectroscopy (EIS) were made using an EG&G Potentiostat Model 273A with model 352 and model 398 softwares. Linear polarization resistance measurements were carried out within ± 20 mV with respect to the corrosion potential (E_{corr}). EIS measurements were performed in the frequency range between 100 kHz and 10 mHz. Sinusoidal voltage of ± 10 mV was supplied, and direct current (DC) potential was set to the corrosion potential.

Galvanic current measurements were conducted with steel/copper and steel/stainless steel sensor systems at ambient temperature and made with a zero-resistance ammeter (Fig. 1).

3. Results and discussion

3.1 Tests in simulated concrete solution

3.1.1 Potentiodynamic polarization test

Fig. 4 shows the potentiodynamic polarization curves of steel, stainless steel and copper in saturated $Ca(OH)_2$ solution. In chloride-free solution, all specimens are passivated due to the high alkalinity ($12<pH<13$) of the pore solution. If steel is coupled to the cathode materials under such conditions, the galvanic current between the anode material and the cathode material will be negligibly low due to the small difference between open-circuit potentials.[8]

Fig. 5 shows the potentodynamic polarization curves of steel, stainless steel and copper in saturated $Ca(OH)_2$ solution with 3.5 wt.% NaCl addition.

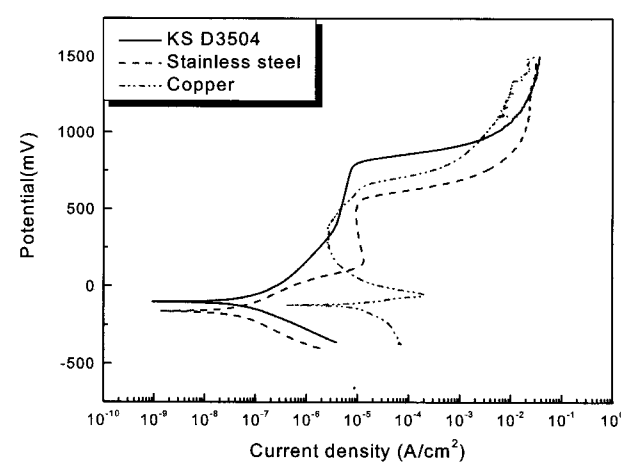

Fig. 4. Polarization curves of specimens in saturated $Ca(OH)_2$ solution.

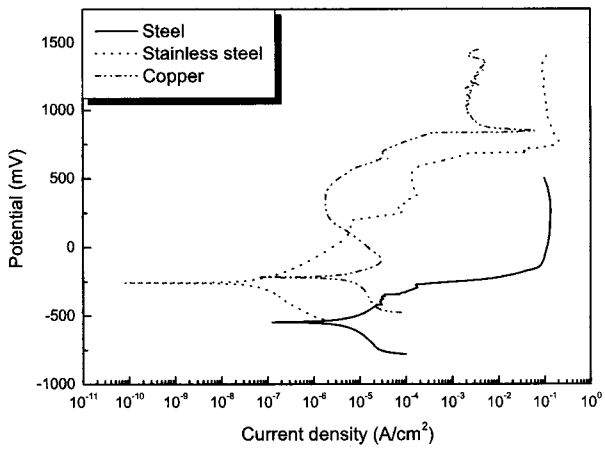

Fig. 5. Polarization curves of specimens in saturated $Ca(OH)_2$ with 3.5 wt.% NaCl solution.

Table 1. Result of corrosion potential and corrosion rate measurements in different solutions.

solution		KS D 3504	Stainless steel	Copper
saturated $Ca(OH)_2$	E_{corr} (mV)	-102	-164	-127
	Corrosion rate (mpy)	0.03	0.01	3.75
saturated $Ca(OH)_2$ with 3.5 wt.% NaCl addition	E_{corr} (mV)	-546	-225	-220
	Corrosion rate (mpy)	1.90	0.04	3.82

Corrosion rate was determined by Tafel extrapolation method. The corrosion current density can be measured and can yield a corrosion rate based on Faraday's law[9]:

$$CorrosionRate(mpy) = \frac{0.13 \times {}_{corr}(\text{¥}A/cm^2) \times E}{Density\ (g/cm^3)} \quad (1)$$

where 0.13 is the metric and time conversion factor and EW is the equivalent weight in grams. Table 1 shows the result of corrosion potential and corrosion rate measured by the Tafel extrapolation method in different solutions. The corrosion rate of all samples increased with existing chloride ions. However, the anodic behavior above the Tafel region is different between stainless steel and copper. The passive film of stainless steel is broken in that region, while, the CuCl film of copper starts to build up on the surface. In the case of copper, the magnitudes of the peak current and the current minimum decrease as the Cl^- concentration increases.[10)-11)] Comparison of the polarization results with and without chlorides indicated the possibility of detecting an ingress point in time of chlorides by measuring the galvanic current between the two metals.

3.1.2 Immersion test

Fig. 6 is a plot of the cumulative weight loss (mg/㎠) of steel (after oxide removal). The weight loss increased rapidly up to 1.5 mg/㎠. With a further increase in the immersion time, a little change in the weight losses was detected. Corrosion rate of the reinforcing steel was determined by using the weight loss method (Fig. 7). The average corrosion rate can be calculated by the following equation (2)[12]:

$$CorrosionRate\ (mpy) = \frac{3.45 \times 1^6 \times Weightloss(g)}{Area(cm^2)\ i\ Density(g/cm^3) \times Time(h)} \quad (2)$$

Initially, corrosion rates decreased with time. Then, corrosion rates maintain a steady state with time. This

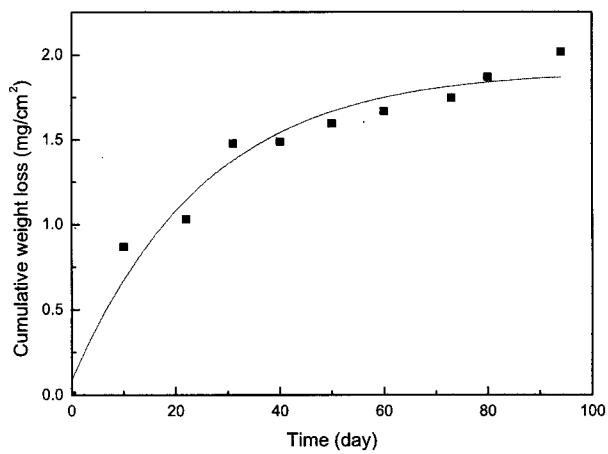

Fig. 6. Weight loss of reinforcing steels in saturated $Ca(OH)_2$ with 3.5 wt.% NaCl solution.

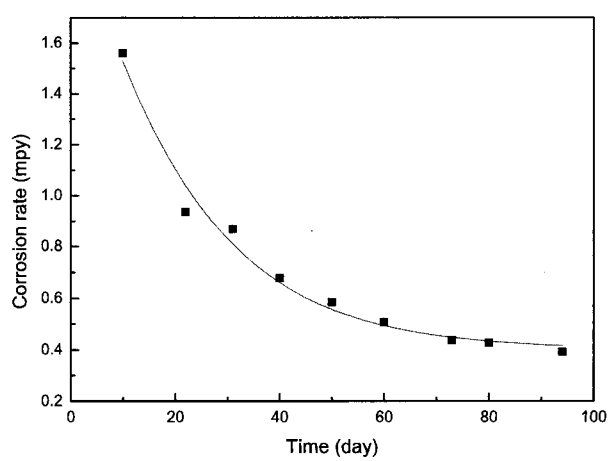

Fig. 7. Corrosion rate of reinforcing steels in saturated $Ca(OH)_2$ with 3.5 wt.% NaCl solution.

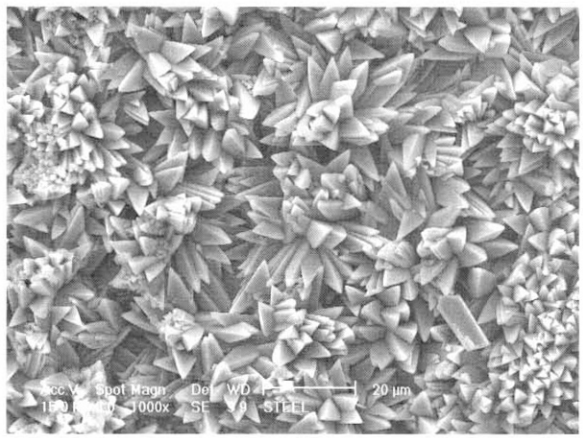

Fig. 8. Surface morphology of the reinforcing steel after the immersion test in saturated $Ca(OH)_2$ solution with 3.5 wt.% NaCl addition.

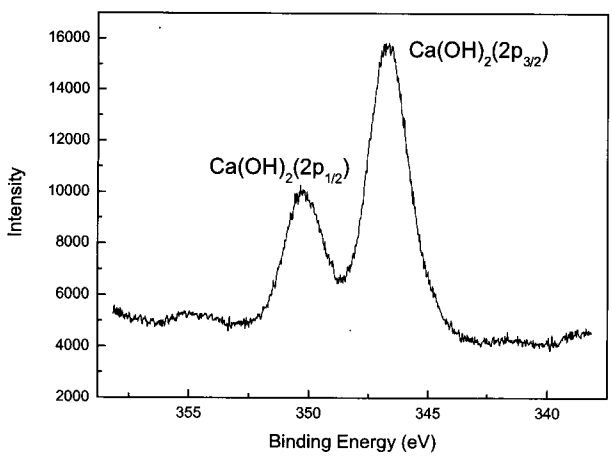

Fig. 9. XPS spectrum of the reinforcing steel after the immersion test in saturated $Ca(OH)_2$ solution with 3.5 wt.% NaCl addition.

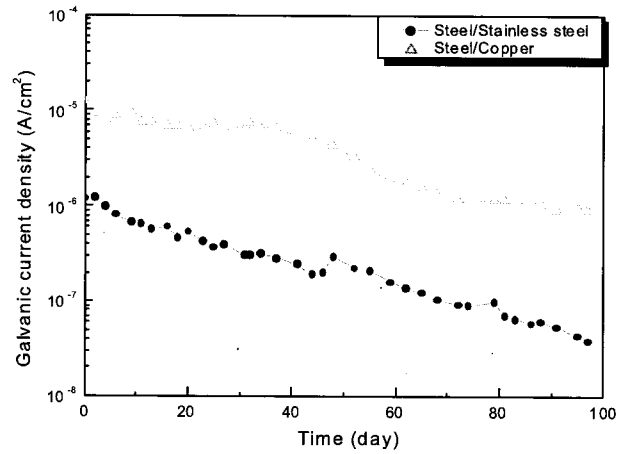

Fig. 10. Galvanic current density versus time in saturated $Ca(OH)_2$ solution with 3.5 wt.% NaCl addition.

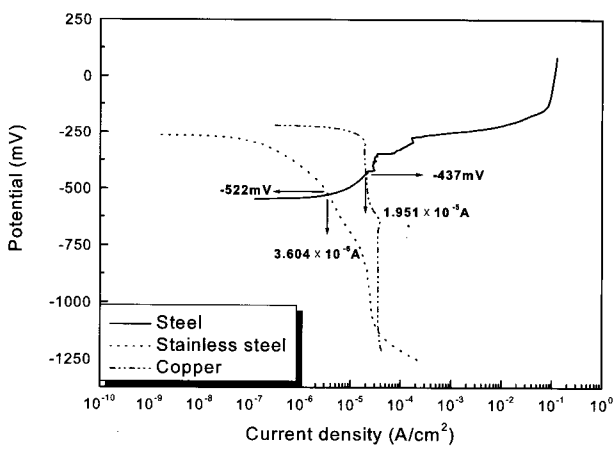

Fig. 11. Anodic polarization curve of reinforcing steel and cathodic polarization curves of stainless steel and copper in saturated $Ca(OH)_2$ solution with 3.5 wt.% NaCl addition.

behavior was closely related to the presence of $Ca(OH)_2$ at the steel surface as shown in Figs. 8 and 9. These Figs. show surface morphology and XPS spectrum of the reinforcing steel after the immersion test, respectively. $Ca(OH)_2$ crystals can restrain a pH drop at the steel surface. The crystals will thus provide protection against steel corrosion.[2)]

3.1.3 Galvanic corrosion test

Fig. 10 shows the galvanic current density versus time. The galvanic current density decreased with time. This observation would be explained on the basis that $Ca(OH)_2$ crystal of specimens restrained a pH drop and reduced the surface area. Generally, if the area of metal is decreased, the curves for both reactions associated with metal (anodic dissolution and cathodic reduction on metal) move to the left or to lower values of current proportional to the decrease in area.[13)] Also, Fig. 10 indicated that the galvanic current density of steel/copper was higher than that of steel/stainless steel. When steel is coupled to cathode materials, that the galvanic current density is high means the steel corrodes at a high rate. This result was consistent with predicting galvanic coupling effects in Fig. 11. According to the polarization curves, the galvanic current in steel/stainless steel is lower than that in steel/copper. Thus, the lifetime of steel/copper sensor is shorter than that of steel/stainless steel sensor. However, it can be assumed that the steel/copper sensor is more suitable for high resistance environment.

Electrochemical reactions either produce or consume electrons. Thus, the rate of electron flow to or from a reacting interface is a measure of reaction rate. Electron flow is conveniently measured as current, I, in amperes,

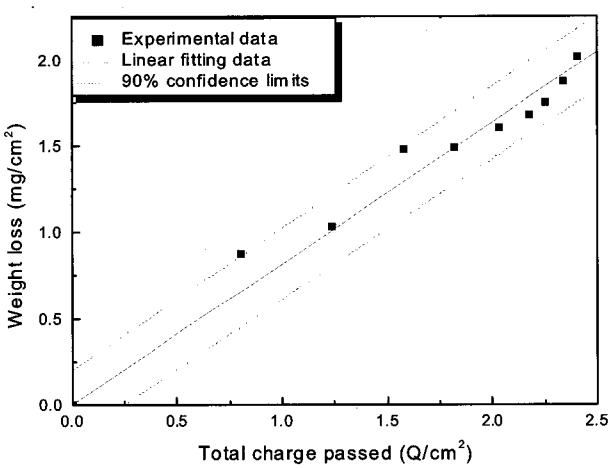

Fig. 12. Weight loss of reinforcing steel and output of sensor system in saturated $Ca(OH)_2$ solution with 3.5 wt.% NaCl addition: (a) steel/stainless steel sensor system, (b) steel/copper sensor system.

where 1-ampere is equal to 1-coulomb of charge (6.25×10^{18} electrons) per second. The galvanic current and time were integrated to the coulomb value based on Faraday's law[14]:

$$Q = I \times t \quad \frac{nFw}{a} \tag{3}$$

where F is Faraday's constant (96,500 coulombs/equivalent), n the number of equivalents exchanged, w the weight loss, a the atomic weight and Q the total coulombs

Fig. 12 shows the correlation between the coulomb values of the sensor system and the weight loss (㎎/㎠) of the reinforcing steel. A good correlation was observed in the two systems. The output of steel/stainless steel sensor system showed a better linear correlation than that of steel/copper. Thus, the steel/stainless steel sensor system is more reliable. The current flows in the galvanic sensor are a representative of what is happening in the steel and how much corrosion on the reinforcing steel of a real structure is occurring. However, the galvanic current can not be detected when the resistance of the concrete is too high to support the galvanic cell. In case the resistance of the concrete is high, the steel/copper sensor can be more effective due to the high galvanic current.

3.2 Tests in real concrete environment

3.2.1 Electrochemical behavior of steel bar

The time-to-corrosion is the time required for chlorides to penetrate the concrete cover in sufficient quantities to initiate corrosion and was determined with corrosion potential. Fig. 13 shows the potential varieties of the steel bar with time. The readings were in the range -250 to -150 mV vs. CSE until 210 days after immersion, corresponding to a state of passivity based on the Pourbaix diagram.[15] After 210 days of exposure, a sharp drop in the corrosion potential was observed, which indicated the initiation of the corrosion process. According to ASTM C 876, if the potential becomes more negative than -350 mV vs. CSE, there is a greater than 90% probability that corrosion of reinforcing steel is occurring.[16]

The R_p evolution obtained from linear polarization resistance measurement for the steel bar is shown in Fig. 14. The readings were higher than 500 $k\Omega \cdot cm^2$ until 210 days of immersion. After that period, a drop in polarization resistance was observed. This resulted in the initiation of corrosion within a few days, as was concluded from the drop of corrosion potential. The corrosion current density (i_{corr}) was calculated using a B value of 26 mV/decade in the equation (4):

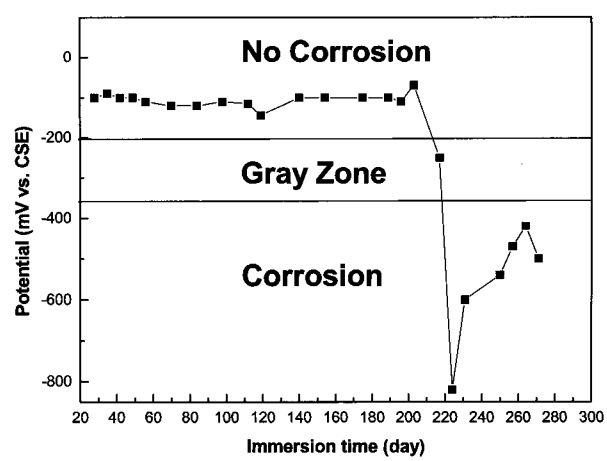

Fig. 13. Open-circuit potential evolution of reinforcing steel in concrete.

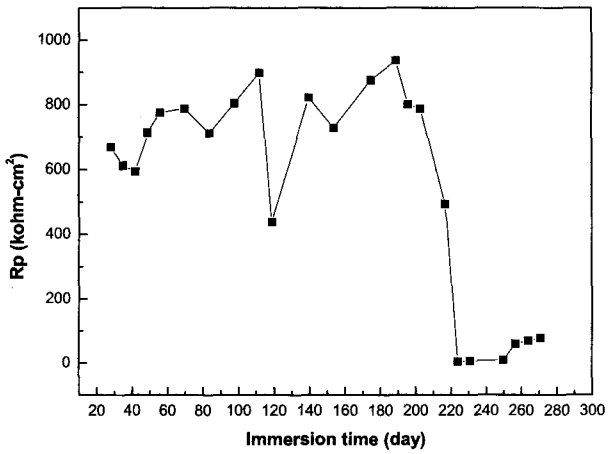

Fig. 14. Rp evolution obtained from linear polarization resistance measurement.

$$i_{corr} = B/R_p \quad (4)$$

and equation (1) were used to calculate the corrosion rate for the steel bar in concrete.[14),17)]

Corrosion rate calculated from the linear polarization resistance measurement was depicted in Fig. 15. After 210 days of immersion, corrosion rate increased significantly, which indicates the onset of the corrosion. Typically, corrosion occurs when corrosion rate is more than 0.24 mpy.[18)]

For better information on the mechanism of the corrosion reaction, impedance measurement was performed. Fig. 16 shows the typical Nyquist plots for the steel bar in concrete. These spectra are constituted by a capacitive arc at experimental frequency region. The shape of spectra with respect to time was similar, but after 210 days with a significant reduction in the diameter of the semicircle corresponding to the charge transfer resistance. The electrical equivalent circuit represented in Fig. 17 was applied to model the EIS data for steel bar. The equivalent circuit consists of the following element: an ionic resistance R_s in the electrolyte filling the pores, a capacitance C_{film} and a resistance R_{film} for surface layer of steel bar; and a capacitance C_{dl} and a charge transfer resistance R_{ct} for steel bar. The presence of depressed semi-circles suggests a non-ideal behavior of the capacitors, leading to the introduction of the constant phase element (CPE) in the equivalent circuits. CPE is widely used in data fitting to allow for depressed semicircles.[19)] The capacitance is replaced with a CPE for a better fit quality. The fitting procedure was performed using a ZsimpWin program. The simulated sum of R_{film} and R_{ct} are presented in Fig. 18. Until 175 days of immersion, the sum of R_{film} and R_{ct} had increased with increasing time, which induced the stable layer on the steel bar surface. After 196 days of exposure, however, the sum of R_{film} and R_{ct} tend to decrease due to onset of breakdown in the passive film.

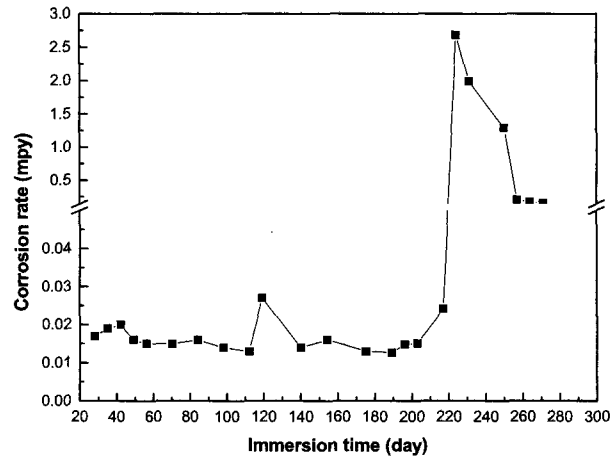

Fig. 15. Corrosion rate of reinforcing steel calculated from linear polarization measurement.

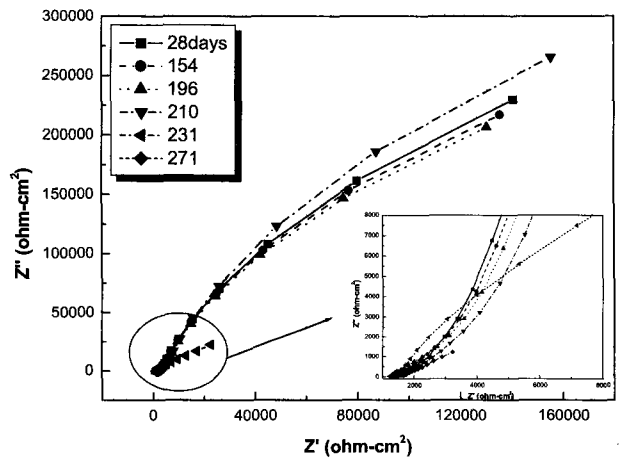

Fig. 16. Impedance spectra in Nyquist plot of reinforcing steel in concrete.

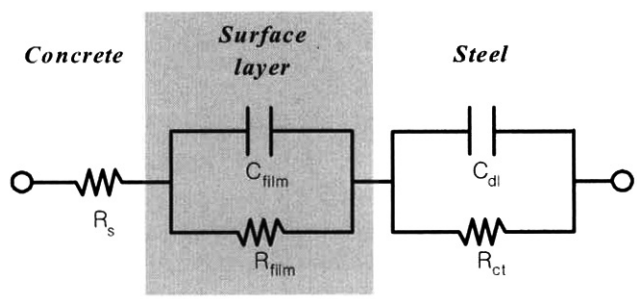

Fig. 17. Equivalent circuit for the corrosion behavior of reinforcing steel in concrete.

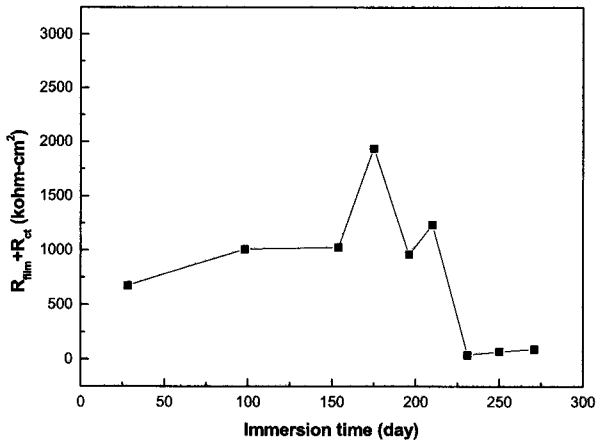

Fig. 18. Sum of R_{film} and R_{ct} vs. immersion time.

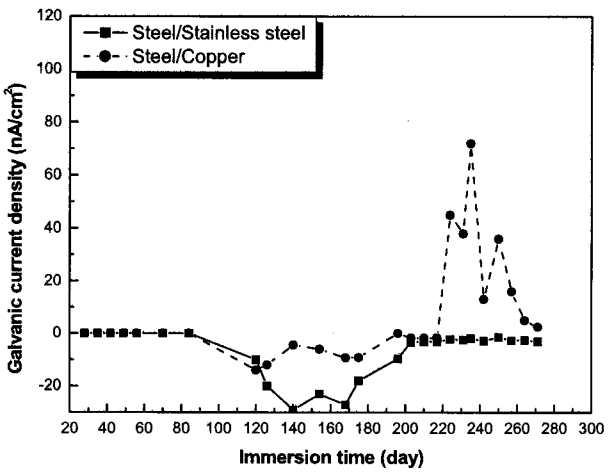

Fig. 19. Galvanic current density versus time.

A drop in the sum of R_{film} and R_{ct} was observed after 210 days. Accordingly, it is considered that corrosion process of steel bar started after 210 days of immersion. This result corresponds to the results of open-circuit potential monitoring and linear polarization resistance measurement.

3.2.2 Galvanic corrosion test of sensor

Fig. 19 shows the galvanic current density obtained from galvanic sensor with time. The galvanic current density maintains a steady state with time close to zero. After 217 days, it was observed that galvanic current density of steel/copper sensor increased significantly. The trend of galvanic current density of steel/copper sensor has a strong resemblance to that of electrochemical behavior of steel bar. However, steel/stainless steel sensor maintains a galvanic current density value of nearby zero at the time of corrosion.

Fig. 20 presents the correlation between the coulomb

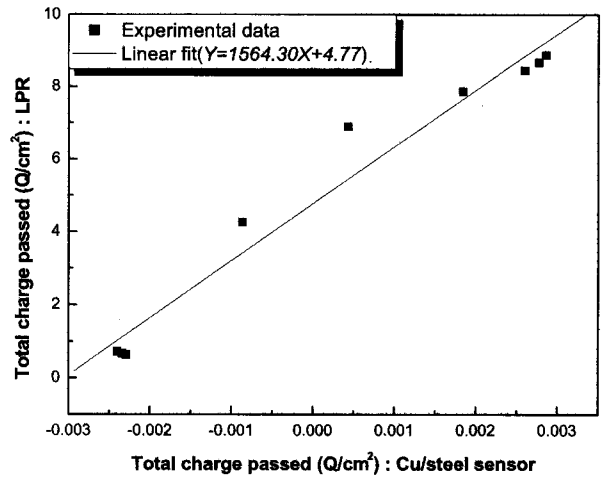

(a)

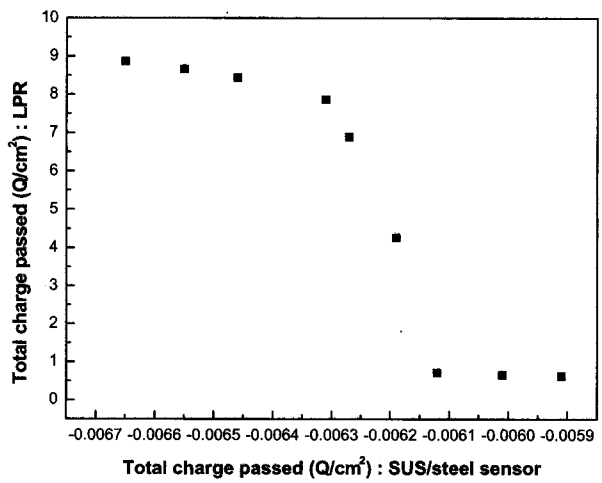

(b)

Fig. 20. The relationship between the charges of reinforcing steel obtained from linear polarization resistance measurement (LPR) and sensor system: (a) steel/copper sensor system, (b) steel/stainless sensor system.

values of the galvanic sensor and the steel bar obtained from linear polarization resistance (LPR) measurement. A good correlation was observed between steel/copper sensor and steel bar. Accordingly, galvanic current of steel/copper sensor makes a detection of corrosion initiation time and corrosion rate. In simulated concrete pore solution, the output of steel/stainless sensor indicated a better linear correlation than that of steel/copper sensor. In concrete environment, however, there is no correlation between steel/stainless steel sensor and steel bar because the resistance of the concrete is too high to support the galvanic current. Therefore, the steel/stainless steel sensor is not suitable for detecting corrosion damage of reinforcing steel in concrete.

4. Conclusions

From this investigation, the following conclusions could be drawn:

1. The steel/copper sensor could provide a useful non-destructive method of determining actual corrosion rate. This was confirmed by electrochemical measurements in concrete.

2. The onset of corrosion could be detected by measuring the galvanic current of steel/copper sensor.

3. The steel/copper sensor is a reliable corrosion detection system in concrete environment. However, steel/stainless steel sensor is not suitable for detecting corrosion damage of reinforcing steel due to the low current output. Through the relationship between the steel/copper sensor output and the corrosion rate of reinforcing steel, onset of corrosion and corrosion rate of the reinforcing steel could reliably be detected.

References

1. J. P. Broomfield, Corrosion of Steel in Concrete, p.22, E & FN SPON, London, 1997.
2. T. Yonezawa, V. Ashworth, and R. P. M. Procter, *Corrosion* **44**, 489 (1988).
3. M. F. Montemor, A. M. P. Simoes, and M. M. Salta, *Cement and Concrete Composites* **22**, 175 (2000).
4. B. Borgard, C. Warren, S. Somayaji, and R. Heidersbach, Mechanisms of Corrosion of Steel in Concrete, ASTM STP 1065, p.174, Philadelphia, 1990.
5. B. Elsener, *Cement and Concrete Composites* **24**, 65 (2002).
6. C. Arya and P. R. W. Vassie, *Cement and Concrete Research* **25**, 989 (1995).
7. J. Gulikers, *Construction and Building Materials* **11**, 143 (1997).
8. M. Raupach and P. P. Schiessl, *Construction and Building Materials* **11**, 207 (1997).
9. S. W. Dean, Handbook on Corrosion Testing and Evaluation, p.171, John Wiley and Sons, New York, 1971.
10. H. P. Lee and K. Nobe, *Journal of Electrochemical Society* **133**, 2035 (1986).
11. A. V. Benedetti, P. T. A. Sumodjo, K. Nobe, P. L. Cabot and W. G. Proud, *Electrochimica Acta* **40**, 2657 (1995).
12. ASTM Standard G31, "Standard Practice for Laboratory Immersion Corrosion Testing of Metals," in 1994 Book of ASTM Standards, vol. 03.02, p.102, West Conshohocken, ASTM, 1994.
13. R. A. Buchanan, Fundamentals of Electrochemical Corrosion, p.164, ASM International, Ohio, 2000.
14. D. A. Jones, Principles and Prevention of Corrosion, p.75, Prentice-Hall, London, 1996.
15. M. Pourbaix, Atlas of Electrochemical Equilibria, NACE, Houston, Texas, 1974.
16. ASTM C 876-91, Standard Test Method for Half-Cell Potentials of Uncoated Reinforcing Steel in Concrete, ASTM, Philadelphia, PA, 1994.
17. C. Andrade and J.A. Gonzalez, *Mater. Corr.* **29**, 515 (1978).
18. N.S. Berke, M.P. Dallaire, M.C. Hicks, and R.J. Hoopes, *Corrosion* **49**, 934 (1993).
19. B.C. Syrett, Electrochemical Impedance and Noise, NACE, Houston, Texas, 1999.